



Numerical Simulation of Flows Induced by Dam Break: Trapezoidal Obstacles and Venturi Configurations

Samira Gouffi^{1)*}, *Tahar Ikni*¹⁾, *Ferhat Merah*¹⁾, *Ali Berreksi*¹⁾, *Lyacine Bennacer*²⁾

¹⁾ Université de Bejaia, Faculté de Technologie, Département d'Hydraulique, Laboratoire de Recherche en Hydraulique Appliquée et Environnement (LRHAE), 06000, Bejaia, Algérie. * Corresponding Author.

E-Mail : samira.gouffi@univ-bejaia.dz; E-Mail: tahar.ikni@univ-bejaia.dz; E-Mail : ferhat.merah@univ-bejaia.dz;
E-Mail : ali.berreksi@univ-bejaia.dz

²⁾ University of Adrar, Laboratory of Energy, Environment and Information System (LEESI), Route Nationale No. 6, 01000, Adrar, Algeria; E-Mail: lyacine.bennacer@univ-adrar.edu.dz

ARTICLE INFO

Article History:

Received: 19/2/2025

Accepted: 24/4/2025

ABSTRACT

The complexity of water flow in open channels increases significantly as the geometry varies, with contractions, expansions, obstructions and slope changes creating non-uniform and undulating free surface profiles. This study aims to simulate such transient flows using the one-dimensional Saint Venant equations, which provide a reliable framework for modeling dam failure scenarios in channels with variable topographies. A numerical model is developed using an explicit finite difference scheme based on the modified Lax-Friedrichs method. The model simulates dam break flows over dry and wet beds, incorporating geometric complexities, such as trapezoidal obstacles and Venturi-like constrictions. Key parameters are investigated, including Courant number, spatial resolution, Manning's roughness coefficient and variations in bed elevation. Validation is carried out by comparing the model with the ideal analytical solution for dam failure, as well as with experimental and numerical results from the literature. In the ideal configuration, the model achieves a relative error of about 1% in water depth. In more complex scenarios, it maintains high accuracy in predicting water depths and flow patterns. These results demonstrate the robustness and effectiveness of the method, making it a valuable tool for hydraulic engineering applications involving flood propagation, obstacle interaction and complex channel design.

Keywords: Dam break, Saint Venant, Lax-Friedrichs, Numerical modeling, Complex geometry.

INTRODUCTION

Dams play a crucial role in the development and well-being of societies by providing water storage, hydropower generation, and flood protection (Ikni et al., 2018; Oğuzhan Güven & Ozgenç Aksoy, 2020). However, despite their many benefits, the failure, either partial or total, of these structures remains a serious concern due to its potential to cause large-scale disasters (Altınbilek, 2002; Annunziato et al., 2024). In densely

populated regions, dam break floods can lead to devastating consequences, including loss of life, infrastructure damage, and severe economic disruptions (Paşa et al., 2023; Al-Ansari et al., 2015; Albu et al., 2020).

Every year, floods affect millions of people and result in billions of dollars of economic losses, emphasizing the critical importance of accurate and timely flood depth estimation to support effective risk management and emergency response operations

(Shatnawi, 2024). In this context, predicting post-failure flow depths and velocities is essential for flood forecasting, early warning systems, and emergency planning (Nema & Desmukh, 2016; Sawai et al., 2019). To this end, dam break scenarios are commonly employed as benchmark tests for evaluating the performance and robustness of numerical schemes, particularly their ability to capture discontinuities, shock waves, and rapidly varying flow conditions (Baghlani, 2011).

Among the physical complexities associated with flood propagation, flow interaction with channel obstacles is of particular importance. Flow analysis involving trapezoidal and Venturi channel obstacles is fundamental in hydraulic engineering due to its direct impact on channel design, flow measurement, and water resource management (Elhakeem, 2017; Welahettige et al., 2017; Delloum, W. et al., 2024). Trapezoidal obstacles are often used to modify flow paths and dissipate energy, while Venturi configurations induce transitions in flow regimes that are critical in both measurement and control systems. Understanding the behavior of unsteady free surface flows in the presence of such geometries is therefore crucial for designing safe and efficient hydraulic structures.

To capture the dynamics of such flows, robust numerical schemes are required. The Lax-Friedrichs scheme is often chosen for dam break simulations, because it provides a reliable, efficient, and stable approach to solving the shallow water equations with discontinuities (Ikni et al., 2021; Sanjoyo et al., 2020). While more accurate high-order methods exist, the Lax-Friedrichs method remains attractive due to its simplicity and robustness, particularly in engineering applications where computational speed and stability are prioritized.

In this study, we propose an improved implementation of the Lax-Friedrichs scheme, modified relative to the version previously used by Magdalena and Eka Pebriansyah (2022), to enhance stability and accuracy in dam break flow simulations. A parametric study is first conducted to assess the influence of key model parameters on the numerical solution. The robustness and applicability of the proposed scheme are then validated through three benchmark test cases: (i) the idealized dam-break problem over a wet bed, (ii) the dam-break problem over a dry bed, and (iii) the dam-break flow interacting with two types of obstacle: a

trapezoidal barrier and a Venturi channel. These test cases were selected for their relevance to real-world hydraulic configurations and their ability to reproduce complex flow phenomena. The overall objective is to demonstrate the model's ability to accurately capture unsteady free surface flows in the presence of strong discontinuities and geometric complexities, contributing to the development of reliable numerical tools for flood risk assessment and hydraulic structure design.

METHODOLOGY

Free Surface Flow Equations

The one-dimensional system of equations, proposed by Adhémar Jean Claude Barré de Saint Venant, is generally applied to express free surface flows (Chaudhry, 2008). This system is made up of two equations of continuity and momentum. For a rectangular section, this system of equations is written as follows (Garcia-Navarro & Vazquez-Cendon, 2000; Lacasta et al., 2017):

• Equation of continuity:

$$\frac{\partial A}{\partial t} + \frac{\partial Q}{\partial x} = 0 \quad (1)$$

• Equation of momentum:

$$\frac{\partial Q}{\partial t} + \frac{\partial}{\partial x} \left(\frac{Q^2}{A} \right) + gA \frac{\partial y}{\partial x} = -gA \frac{\partial Z_B}{\partial x} - gAJ \quad (2)$$

with, $A = Bh$: the cross-sectional area of the channel (B: width of the channel and h: water height) and $J = \frac{Q|Q|n^2}{A^2RH^{4/3}}$ representing the friction (n Manning's coefficient, and Q standing for the flow rate).

These two equations can be written in the following form:

$$\frac{\partial V}{\partial t} + \frac{\partial F_1}{\partial x} + gA \frac{\partial F_2}{\partial x} = S \quad (3)$$

where,

$$V = \begin{pmatrix} A \\ Q \end{pmatrix}; F_1 = \begin{pmatrix} Q \\ \frac{Q^2}{A} \end{pmatrix}; F_2 = \begin{pmatrix} y \\ Z_B \end{pmatrix}; S = \begin{pmatrix} 0 \\ -gA \frac{\partial Z_B}{\partial x} - gAJ \end{pmatrix}.$$

In this last relationship, V is the vector of conservative variables; F1 (Q) denotes the flow vector; F1 (y) represents the water height; Z_B is the channel bottom elevation, and S is the source vector.

Finite Difference Method

The finite difference method is a well-known method in hydraulics and fluid mechanics. This method involves determining the values of the required function, f , at a few specific points. In the case of solving the Saint Venant equations, a grid in the plane (x, t) is added in order to obtain meshes of size $(\Delta x, \Delta t)$, where Δx and Δt are the space steps and the time steps, respectively.

To solve the one-dimensional Saint Venant system, the first order Lax-Friedrichs scheme was selected due to its simplicity, robustness, and inherent numerical dissipation, which makes it particularly suitable for stabilizing the solution of hyperbolic conservation laws, especially in the presence of sharp gradients or discontinuities, such as shock waves.

A key criterion to ensure the stability of explicit finite difference schemes, like the Lax-Friedrichs scheme, is the Courant–Friedrichs–Lewy (CFL) condition. This condition ensures that information does not travel faster than the numerical domain allows and is expressed as:

$$CFL = \frac{\Delta t \max(|u| + \sqrt{gh})}{\Delta x} < 1 \tag{4}$$

Satisfying this condition is essential for maintaining both stability and convergence of the numerical solution.

A comparative study between the first-order finite difference Lax-Friedrichs numerical scheme and the modified first-order Lax-Friedrichs scheme will be conducted in this work to numerically solve the one-dimensional Saint Venant system.

Lax-Friedrichs Numerical Scheme

The formulation of the Lax-Friedrichs scheme given by Magdalena and Eka Pebriansyah (2022) is written as follows:

$$V_i^{n+1} = \frac{V_{i+1}^n + V_{i-1}^n}{2} - \frac{\Delta t}{2\Delta x} [F1_{i+1}^n - F1_{i-1}^n] - \frac{\Delta t}{2\Delta x} Ag[F2_{i+1}^n - F2_{i-1}^n] + \Delta t S_i^n. \tag{5}$$

This scheme was modified by Saikia and Sarma (2006) by adding an artificial viscosity θ . Then:

$$\left\{ \begin{aligned} V_i^{n+1} &= (1 - \theta)V_i^n + 0.5\theta(V_{i+1}^n + V_{i-1}^n) - \frac{\Delta t}{2\Delta x} [F1_{i+1}^n - F1_{i-1}^n] \\ &\quad - \frac{\Delta t}{2\Delta x} gA[F2_{i+1}^n - F2_{i-1}^n] + \Delta t S_i^n. \end{aligned} \right. \tag{6}$$

$0 \leq \theta \leq 1$

This scheme works well with a value of θ close to one.

Lax-Friedrichs Numerical Scheme of the Present Model

Modifications have been made to better capture the discontinuities, such as shock fronts and rarefaction waves, to improve accuracy and reduce numerical diffusion while preserving the simplicity of the initial approach. Two major modifications have been introduced compared to the classical formulation. These

adjustments aim to capture these discontinuities more effectively, enhance accuracy, and reduce numerical diffusion. The main modifications are as follows:

- Addition of an Artificial Viscosity Filter to the Flux Term;
- Separate Treatment of the Source Term.

First, the numerical flux has been modified by adding an artificial viscosity filter to the classical Lax-Friedrichs formulation. The numerical formulation of the present model using the Lax-Friedrichs scheme is written as:

$$\left\{ \begin{aligned} V_i^{n+1} &= (1 - \theta)V_i^n + 0.5\theta(V_{i+1}^n + V_{i-1}^n) - \frac{\Delta t}{\Delta x} [(1 - \theta)(F1_i^n - F1_{i-1}^n) + \theta(F1_{i+1}^n - F1_i^n)] \\ &\quad - \frac{\Delta t}{\Delta x} gA[(1 - \theta)(F2_i^n - F2_{i-1}^n) + \theta(F2_{i+1}^n - F2_i^n)] + \Delta t S_i^n. \end{aligned} \right. \tag{7}$$

$0 \leq \theta \leq 1$

Second, the source term (S) plays a key role in accurately capturing physical effects, such as bed slope and frictional resistance. The discretization of source terms in the Saint Venant equations is an essential step

in guaranteeing the accuracy and stability of numerical schemes, as proposed by Huang and Song (1985), in order to effectively reduce numerical instabilities and improve computational robustness, especially in

complex flows (Garcia-Navarro et al., 1999). The new formulations of the friction slope J and the source term S are:

We have: $J = \frac{Q|Q|n^2}{A^2RH^{4/3}}$ posing $J = \frac{ARH^{2/3}}{n}$ then, the

new formulation of J: $J = \frac{Q|Q|}{K^2}$

$$(J)_i = \left(\frac{Q}{K^2}\right)_i^n (\theta Q_i^{n+1} + (1 - \theta)Q_i^n) \tag{8}$$

$$S_i^n = \left(\begin{matrix} 0 \\ -gA_i^n \frac{\partial z_B}{\partial x} - gA_i^n \left(\left(\frac{Q}{K^2}\right)_i^n (\theta Q_i^{n+1} + (1 - \theta)Q_i^n) \right) \end{matrix} \right) \tag{9}$$

One of the most commonly used techniques for dealing with boundary conditions in numerical simulations is linear extrapolation. This method consists of estimating the boundary values from the interior values obtained at previous time steps, thus ensuring both continuity and numerical stability. For example, given the interior values V_{N-2}^{n+1} and V_{N-1}^{n+1} computed at time t^{n+1} , the boundary values V_N^{n+1} and V_{N+1}^{n+1} can be estimated using the following linear extrapolation formulae (Ikni et al., 2021):

$$\begin{cases} V_1^{n+1} = 2V_2^{n+1} - V_3^{n+1} \\ V_N^{n+1} = 2V_{N-1}^{n+1} - V_{N-2}^{n+1} \end{cases} \tag{10}$$

with, $V = \begin{pmatrix} A \\ Q \end{pmatrix}$ is the flow vector composed of the transverse water surface and the flow rate.

This method is widely validated in literature. Das and Bagheri (2015) have demonstrated the method's robustness in hydro-dynamics modeling. This technique remains a reference choice due to its simplicity, efficiency, and the ease which it integrates into explicit schemes for solving Saint Venant equations. The overall numerical procedure adopted to solve the shallow water equations for the dam break simulation is summarized in the flowchart shown in Figure (1).

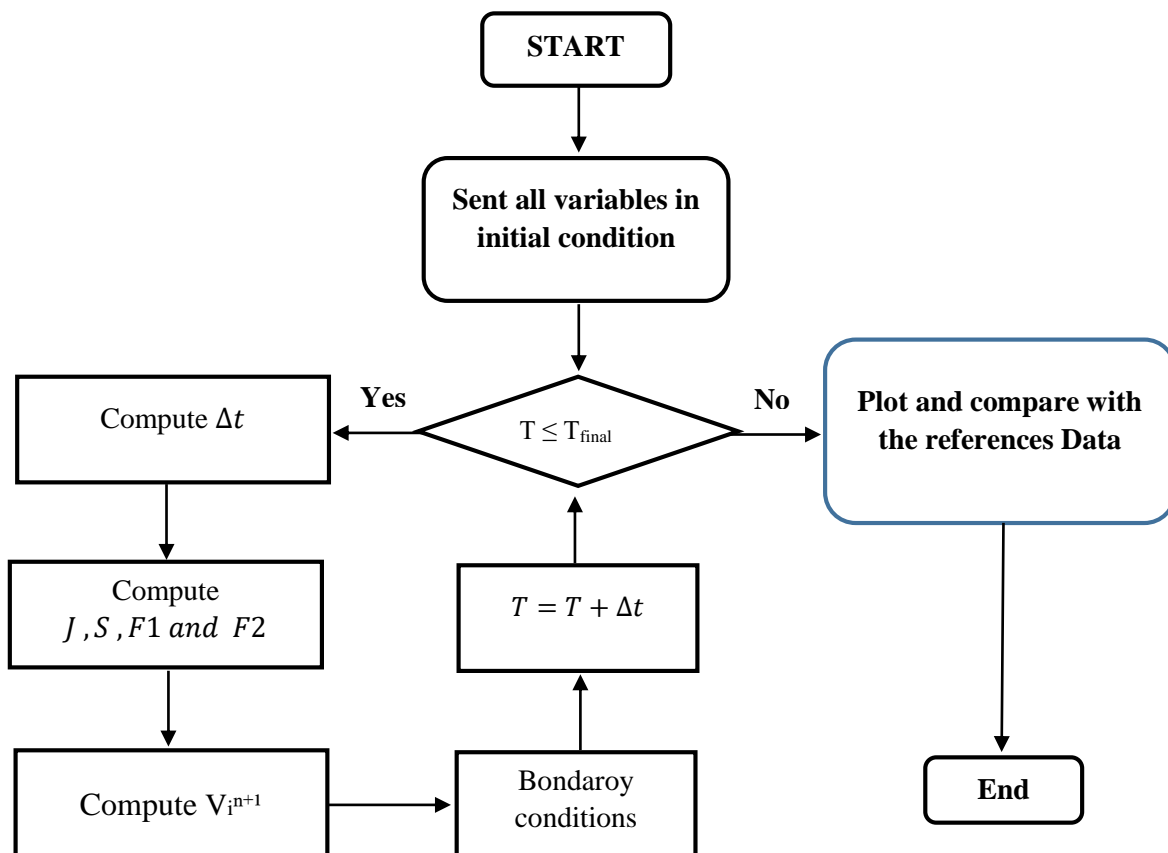


Figure (1): Flowchart of the numerical procedure for simulating dam break

Numerical results of the developed model

A preliminary comparison was performed between the developed model and the classical Lax-Friedrichs scheme, as implemented by Magdalena and Eka Pebriansyah (2022), to evaluate the potential improvements in accuracy and robustness. Subsequently, a parametric study was conducted to examine the influence of key simulation parameters. Based on the findings of this sensitivity analysis, a series of validation tests were carried out to further assess the model's performance. The first validation case corresponds to an idealized dam break scenario with instantaneous and complete failure in a horizontal channel. The second test introduces a trapezoidal obstacle to investigate the model's capability in simulating flow-structure interactions. The third scenario involves a more complex geometry, with a

contracted-expanded channel section and a dry, rough bed, aimed at evaluating the model under realistic flow conditions. Together, these benchmark cases provide a comprehensive evaluation framework for assessing the accuracy and applicability of the proposed numerical approach.

Idealized Dam Break Flow Problem Over a Wet Bed

This test investigates the flow generated by a dam break positioned in the middle of a horizontal channel ($x=L/2$), where the total channel length is $L=200$ m. Initial water levels are defined as $h_a=10$ m upstream and $h_r=1$ m downstream of the dam location (Figure (2)). A structured mesh consisting of 800 nodes is used for the numerical simulations. This scenario has been previously analyzed by Magdalena and Eka Pebriansyah (2022).

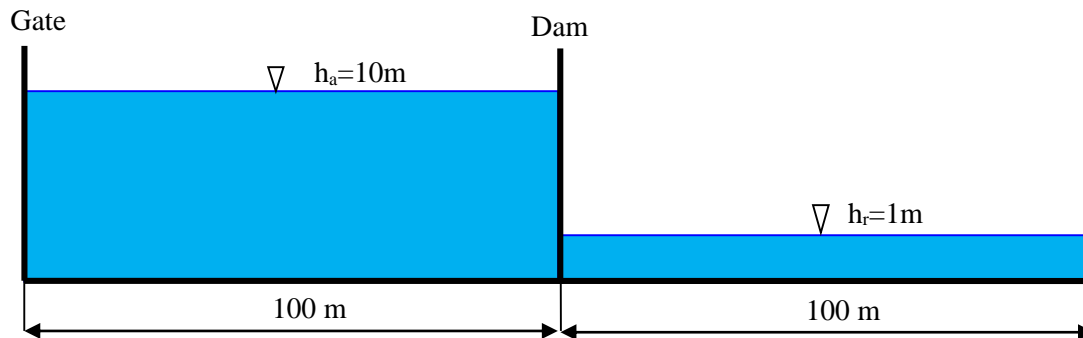


Figure (2) : Ideal dam break on a wet bed

This test is used to check the robustness of the modified Lax-Friedrichs numerical scheme for describing the dam break wave in a horizontal rectangular channel. Figure (3) shows, respectively, the analytical and numerical simulation results at $t=5$ s after the dam break.

According to Figure (3a), it can be observed that the numerical simulation obtained results with the modified model converge with the analytical solution of Stoker. The results show that the new formulation of the term flux (Eq. (7)) gives better simulations.

Figure (3b) and Figure (3c) present a comparison of the analytical and numerical findings for flow velocity and flow rate at $t=5$ s after the dam failure. The numerical results are observed to closely align with the analytical solutions provided by Stoker (1957). Figure (3b) shows that the velocity increases rapidly after the dam break, reaching a constant peak between approximately 90 m and 150 m before declining sharply. This behavior

aligns with the propagation of a shock wave in free surface flow, demonstrating the model's accuracy in capturing the dam break phenomenon. Figure (3c) indicates that the flow rate distribution exhibits a similar trend to the velocity, with a rapid increase followed by a period of stability before decreasing. The close correspondence between the curves validates the model's ability to accurately capture the wave dynamics and flow characteristics.

Assessment of the Relative Error

To assess the accuracy of the dam break simulation proposed model, Magdalena and Eka Pebriansyah (2022) performed a relative error analysis in comparison with the analytical solution of Stoker (1957). In order to quantitatively assess the overall performance over the entire computational domain, the relative error (E_{rr}), as defined by LeVeque (1992), was used.

$$E_{rr} = \sqrt{\frac{\sum_i^n (h_{A,i} - h_{N,i})^2}{\sum_i^n h_{A,i}^2}} \quad (11)$$

Here, (h_A) is the water height in the analytical solution and (h_N) is the water height in the numerical solution. This calculation allows the quantification of the difference between the values predicted by the proposed model and those considered as references, thus

determining the model's effectiveness in faithfully reproducing flow dynamics. Measuring the relative error provides valuable information for judging the robustness of our approach, particularly in complex simulation conditions where accuracy is crucial for water infrastructure management, risk management, and risk-management applications.

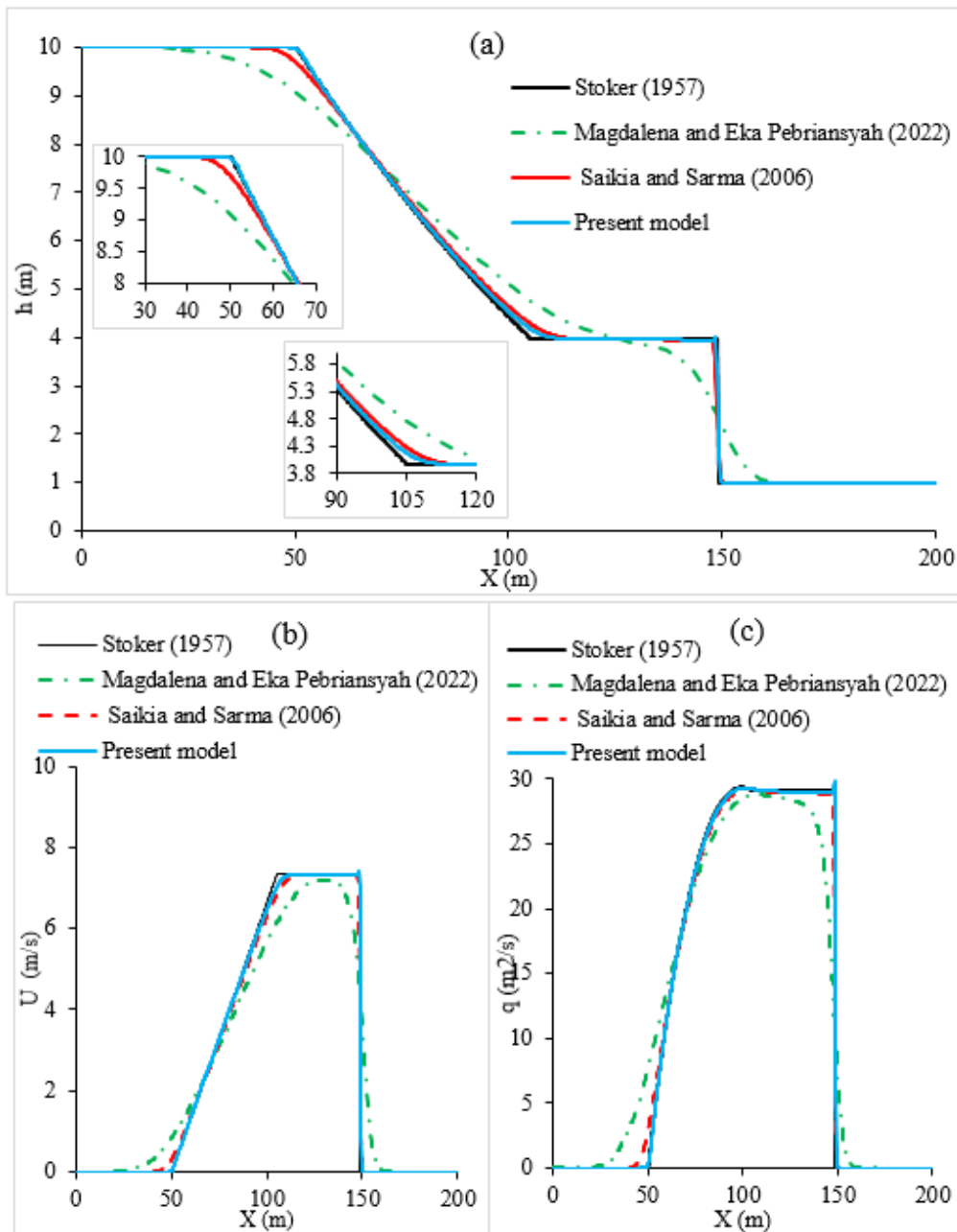


Figure (3): Analytical and simulated results of dam break on a wet bed:
a) Water height h(m); b) Flow velocity; c) Flow rate

Table 1. Relative error results in wet conditions, with a downstream height equal to 1m

Numerical schemes	Water height error	Velocity rate error	Flow rate error
Magdalena and Eka Pebriansyah (2022)	0.8738	0.164148	0.1658
Saikia and Sarma (2006)	0.0170	0.0518	0.0491
Present model	0.0103	0.0442	0.0257

The analysis of relative errors (Table 1) shows that the Lax-Friedrichs scheme, applied with the modifications of Equation (7), offers improved accuracy for dam failure simulation, particularly for water heads. Compared with the initial version of the scheme, this modified approach significantly reduces the errors for the key parameters of head (h), velocity (U), and discharge (Q). For water depth, the relative error is approximately 1%. These results underline the robustness and reliability of the model in reproducing complex flow phenomena during dam breach, making it promising for more advanced applications in hydraulic infrastructure management and flood risk prevention.

Parametric Study

Variation of Courant-Friedrichs-Lewy (CFL) Number and the Spatial Step Size (Δx)

The objective of these tests is to determine appropriate values for the spatial step size (Δx) and Courant-Friedrichs-Lewy (CFL) number to ensure the stability of the modified scheme (Eq. 7). To assess its robustness, a dam break scenario was simulated with an upstream water height of 10 m and a downstream water height of 1 m, yielding a depth ratio $\alpha = 0.1$. The numerical results were compared with Stoker solution (1957), using a fixed step size $\Delta x=0.25$ m and a total simulation duration of 5 seconds (Figure (4)).

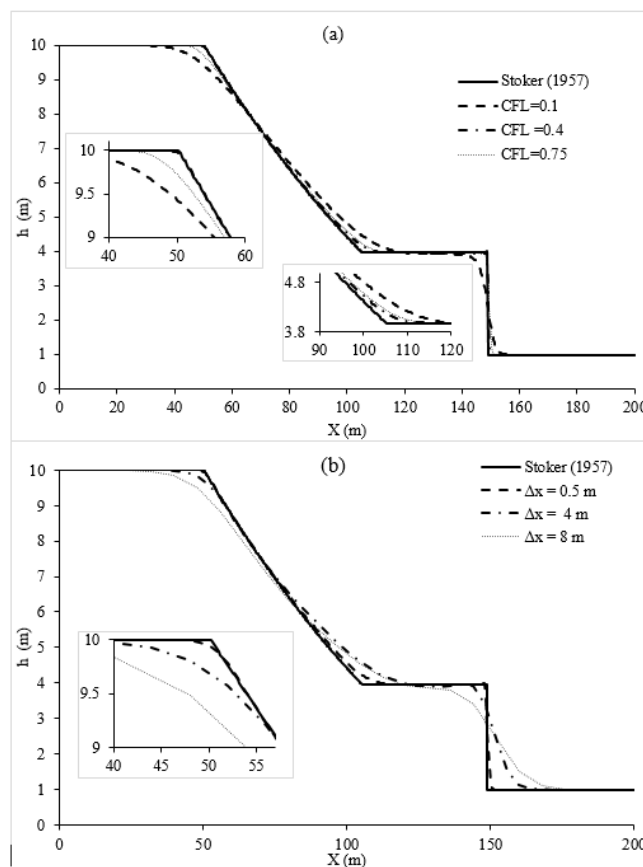


Figure (4): Effects of CFL number and spatial step on flow simulation compared to analytical solution

Figure (4a) illustrates the effect of the Courant-Friedrichs-Lewy number on simulation accuracy. At low CFL number values (0.1), excessive numerical damping leads to a smoothed representation of the shock. As the CFL number increases (0.75), the numerical solution aligns more closely with the analytical one. These results underline the need for an optimal CFL number value that ensures both numerical stability and solution accuracy in transient flow simulations.

Figure (4b) shows the comparison between Stoker's solution and numerical results for various spatial step sizes Δx . Finer resolutions ($\Delta x = 0.5$ m) provide more accurate results, closely capturing the shock and rarefaction waves. As Δx increases (to 8 m), numerical diffusion becomes more pronounced, and the solution deviates from the analytical profile. This highlights the importance of mesh refinement in accurately resolving flow discontinuities in dam break problems.

Variation of Manning's Roughness Coefficient (n) and Channel Topography (z)

To better understand the dynamics of dam break

flows, it is essential to investigate the influence of key physical parameters on the flow behaviour. In this study, we focus on the effects of Manning's roughness coefficient and channel topography on the water depth and velocity profiles. The roughness coefficient represents the frictional resistance of the channel bed, while the topography defines the geometry through which the flow propagates. A series of numerical tests are carried out, and the results compared with Stoker solution (1957) to validate the model under ideal and more realistic conditions (Figure (5)).

The results of the numerical simulation at time $t = 5$ s are presented in Figure (5a) and Figure (5b). The influence of bed friction is analyzed by varying the Manning roughness coefficient with values $n = 0.00, 0.02, 0.04,$ and 0.06 . As expected, increasing the friction coefficient results in a noticeable deceleration of the flow. This reduced flow velocity leads to a corresponding increase in water depth (see Figure (5a) and Figure (5b)). These observations indicate that higher roughness values dampen the flow momentum, resulting in slower water propagation and elevated water levels behind the wave front.

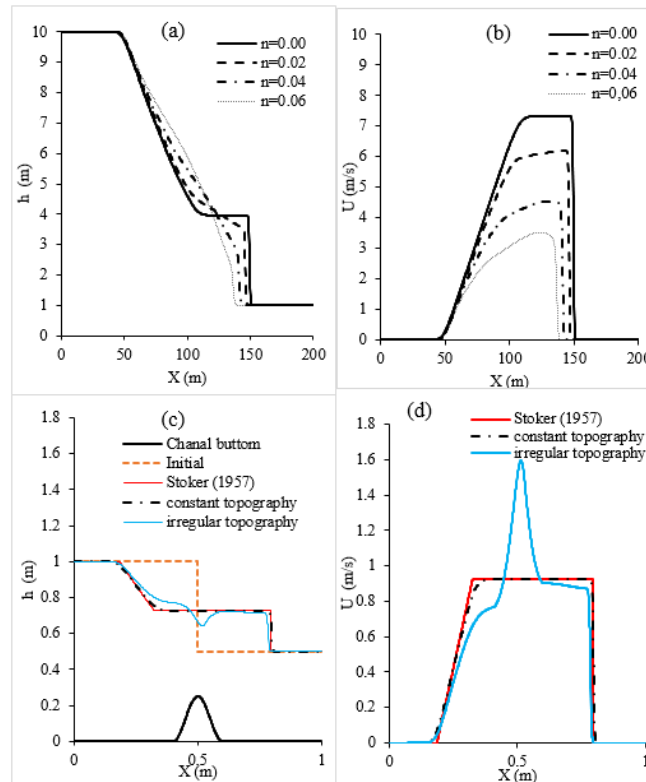


Figure (5): Effect of Manning's roughness coefficient and topographic variations on water depth and velocity profiles during dam break flow, with comparison to analytical solution

Figure (5c) and Figure (5d) show three configurations: a constant topography profile, an irregular topography and an idealized analytical case based on Stoker's (1957) solution. The results show that an irregular topography significantly alters the flow structure, inducing local oscillations and affecting both the shape and velocity of the wave front. Compared to the case of a constant bottom, the presence of topographic irregularities introduces perturbations that are reflected in both the water surface and the bed profile.

The results confirm the robustness and predictive ability of the proposed model for simulating free surface flows under varying roughness conditions and irregular topographies.

Variation of the Ratio (α)

The study of the effect of the ratio (α), defined as the downstream height to the upstream height ration, is essential for understanding the dynamics of flow regimes in dam failure situations. This ratio enables the characterization of different flow states, in particular by determining whether the regime is fluvial, torrential or critical. The variation of the ratio (α) allows for the observation of the transition between these states and the

assessment of the impact of downstream head on flow parameters.

$$\alpha = \frac{h_r}{h_a} \tag{12}$$

The obtained results show that the numerical model, using the modified Lax-Friedrichs scheme, is particularly effective in simulating varied flow regimes and capturing the complex flow associated with the transition between fluvial and torrential regimes. Indeed, in the simulations, the Lax-Friedrichs scheme shows excellent accuracy in representing profiles of head h , velocity (U), Froude number (Fr) and unit flow when comparing numerical results with Stoker's solution for each ratio (α) ((Figure (6)).

When $\alpha = 0.01$, the model simulates a torrential regime with high velocity (Figure (6b)) and a Froude number exceeding one (Figure (6c)), indicating unstable and rapid flow typical of a dam break scenario with a steep downstream gradient. In contrast, when $\alpha = 0.5$, the model reproduces a stable river regime with a Froude number below one (Figure (6.c)), where the relatively high downstream water depth reduces kinetic energy and stabilizes the flow.

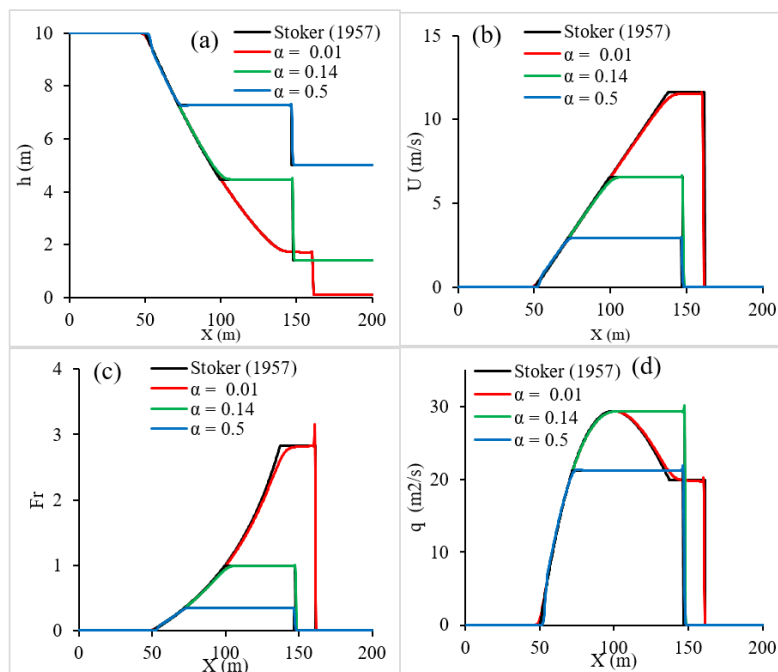


Figure (6): Flow parameters for CFL=0.75 and each depth ratio (α):
a) Water height h (m); b) Flow velocity U (m/s); c) Froude number Fr ;
d) Flow rate per unit width $q = hu$ (m²/s) at $t=5s$

The critical case, with $\alpha=0.14$, presents an intermediate situation where the Froude number is close to one (Figure (6.c)). This critical ratio between upstream and downstream heights enables the model to represent a state of transition between fluvial and torrential regimes. This accuracy in capturing transitional dynamics is crucial for realistic dam break simulations, where the nature of the flow can rapidly change according to topographical variations and hydraulic conditions.

The robustness of the model developed is thus reflected in its ability to simulate a variety of flow regimes accurately, and to reproduce critical transition points, offering a reliable method for studying complex dam break flow phenomena. These results validate the effectiveness of this modified scheme for practical applications in hydraulics.

Idealized Dam Break Flow Problem over a Dry Bed

To assess the ability of the proposed model to accurately predict the propagation of the wave front in real dam break scenarios, the simulation results are compared with the experimental data of Townson and Al-Salihi (1989) and the numerical results of Mohapatra and Bhallamudi (1996) and Das and Bagheri (2015). These experiments were performed in a horizontal rectangular channel 4 m long and 0.1 m wide, in which friction effects were neglected. The upstream and downstream lengths of the channel are 1.8 m and 2.2 m, respectively, with an initial water depth of 0.1 m upstream. Two different ratios were considered in the experiments: $\alpha = 0.0025$ and $\alpha = 0.00001$.

Figure (7a) shows the free surface profiles at $t = 1.5$ s for the case $\alpha = 0.0025$. These profiles include the experimental measurements of Townson and Al-Salihi (1989) and the numerical results of Das and Bagheri (2015), as well as the simulation of the present model. Das and Bagheri (2015) applied second-order and

fourth-order MacCormack schemes to solve the 2D Saint Venant equations. To minimize the spurious oscillations associated with these schemes, they incorporated a dissipative term proposed by Helfrich (1999). In both studies, the spatial discretisation step was $\Delta x = 0.05$ m with a CFL number of 0.57. In the present study, a similar spatial resolution ($\Delta x = 0.05$ m) is used with a CFL number of 0.95 for the Lax-Friedrichs scheme. The agreement between the simulated and experimental results is satisfactory. In particular, the newly formulated Lax-Friedrichs scheme (Eq. (7)) demonstrates strong abilities to capture wave front propagation.

Figure (7b) shows the water surface profiles for the second case ($\alpha = 0.00001$), comparing the experimental data of Townson and Al-Salihi (1989), the numerical results of Mohapatra and Murty Bhallamudi (1996) and those obtained from the present model (Eq. (7)). Mohapatra and Murty Bhallamudi used the MacCormack finite difference scheme with a CFL number of 0.85. Although the wave front height is well predicted in the study, the wave front position is less well predicted. At $t = 1.5$ s, the flow reaches the downstream end of the channel, as clearly shown in Figure (7b). Both the experimental data and the current model results accurately represent the position of the wave front, with excellent agreement between the two.

Dam Break on a Horizontal Plane with the Presence of a Trapezoidal Obstacle

This experiment was carried out by Ozmen-Cagatay and Kocaman (2011). The test bench consists of a channel 9 m long, 0.3 m wide and 0.34 m high. The dam is located at a distance of 4.65m from the channel beginning, and the initial water depth behind the gate is 0.25m. The bed is dry downstream of the dam. A trapezoidal obstacle is placed downstream of the dam at a distance of 1.53m. The downstream end of the channel is open (Figure (8)).

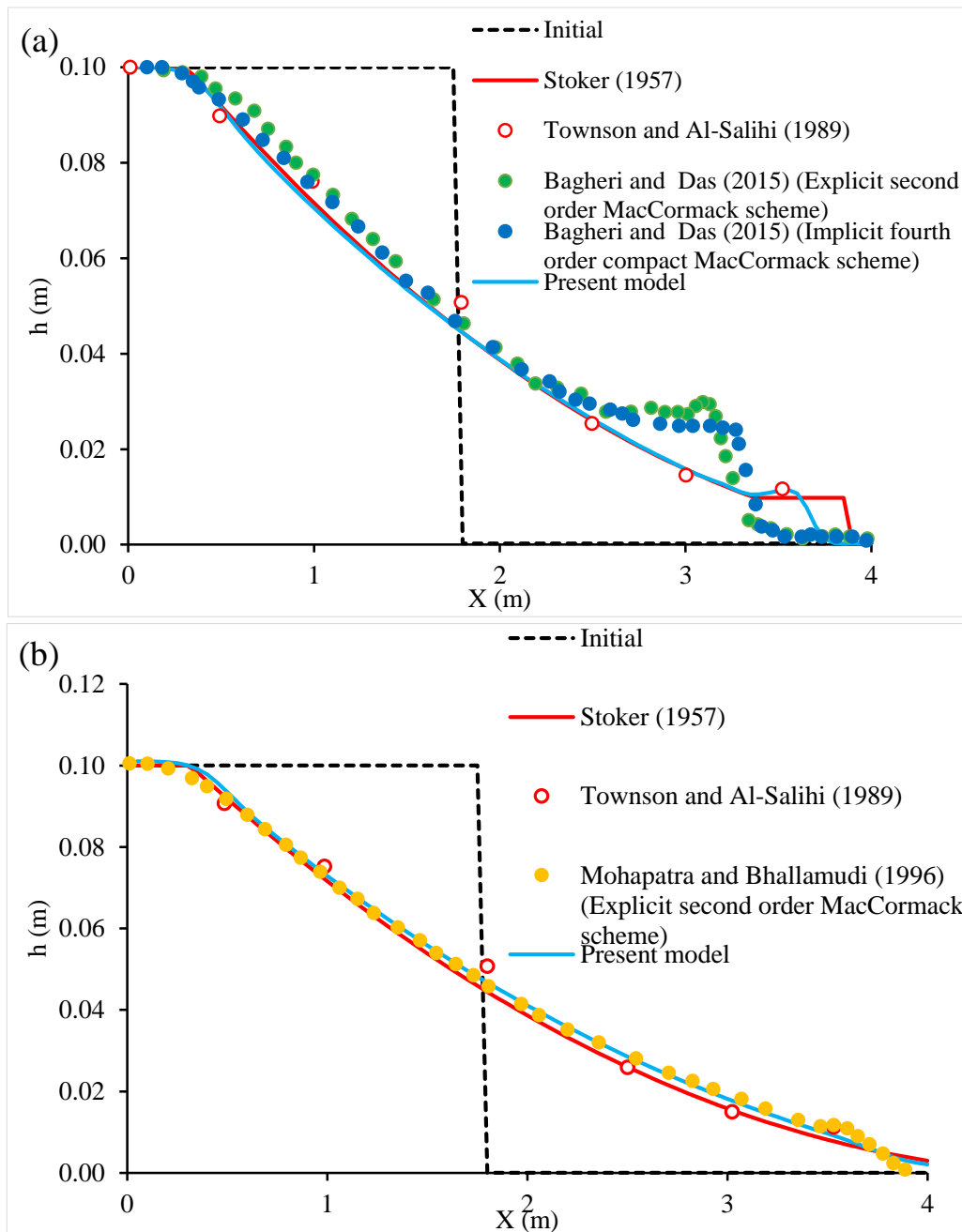


Figure (7): Free surface profile of dam failure at $t=1.5s$ for: a) $\alpha=0.0025$; b) $\alpha=0.00001$

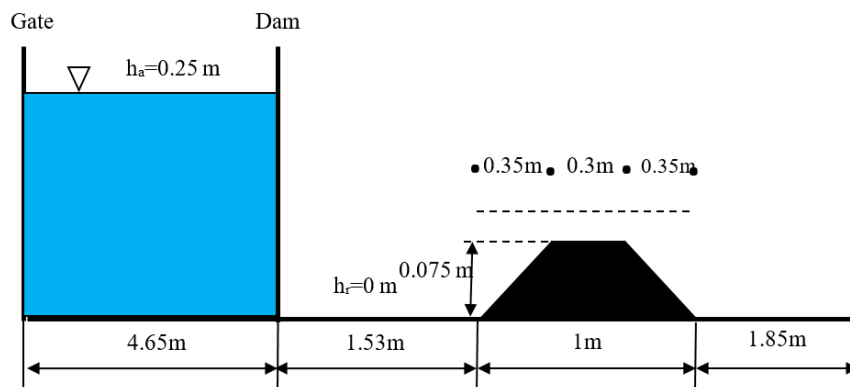


Figure (8): Dam break on a horizontal plane with the presence of a trapezoidal obstacle

Figure (9) shows the experimental results of Ozmen-Cagatay and Kocaman (2011), the numerical results of Magdalena and Eka Pebriansyah (2022) and the results obtained with the present model (Eq. (7)). The same Δx discretization step is used ($\Delta x = 0.25$ m) with a CFL number of 0.75. Figures (9a), (9b), (9c) and (9d) clearly illustrate good calibration between simulated and experimental obtained results. These results prove that

the new model (Eq. (7)) is better than those obtained by Magdalena and Eka Pebriansyah (2022).

Figure (10) shows the variation in water height as a function of time in the channel with the presence of a trapezoidal obstacle. Figure (10a) clearly shows that the flow is before the obstacle at $t=0.84$ s. At $t=1.4$ s, the flow covers the entire obstacle. The dam break wave reaches the downstream end at time $t=2.25$ s.

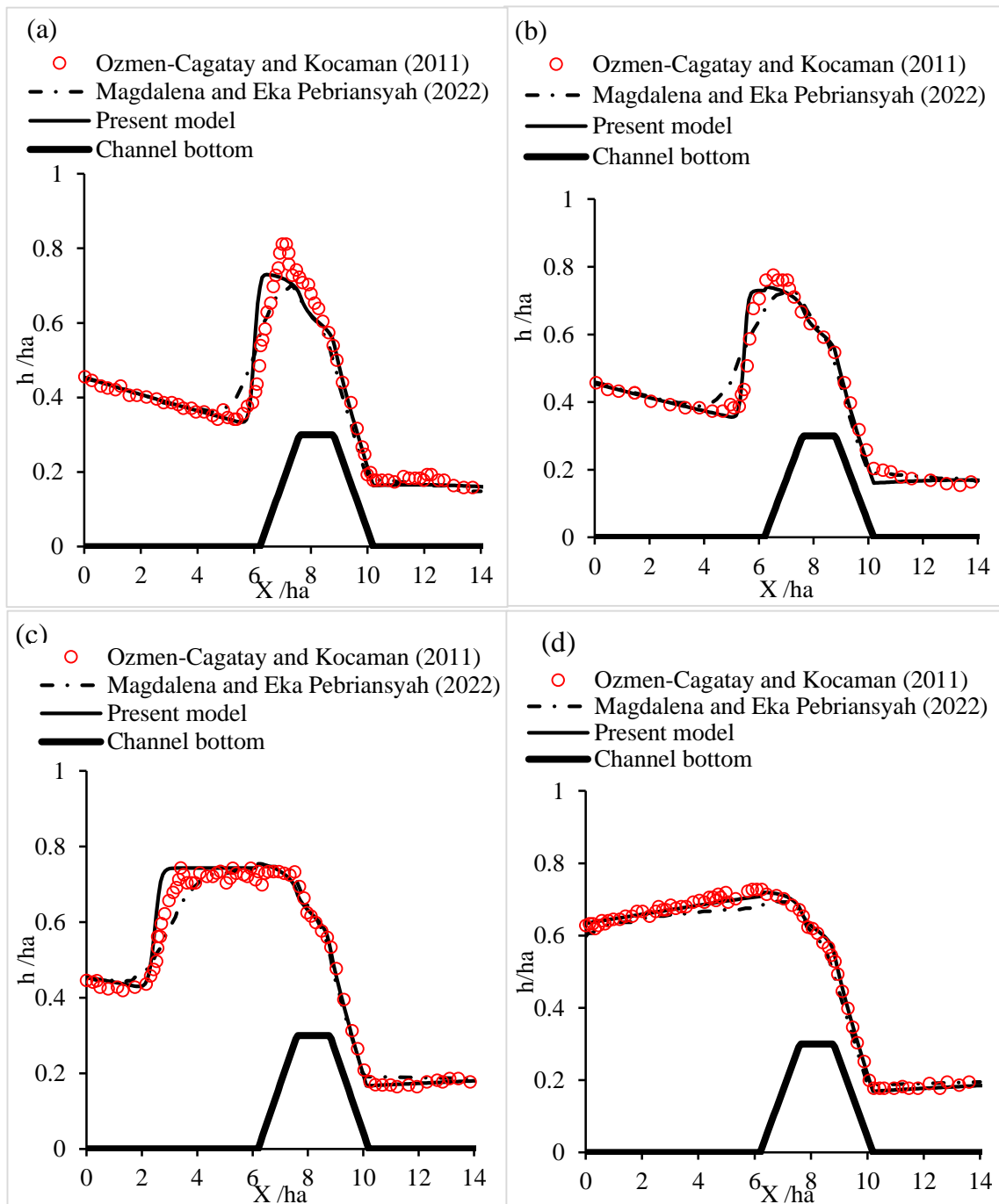


Figure (9): Experimental and simulated results of dam break on a horizontal plane with the presence of a trapezoidal obstacle: a) $t = 2.8$ s; b) $t = 3.3$ s; c) $t = 4.7$ s; d) $t = 6.7$ s

Figure (10) illustrates well the displacement of the wave front in the channel as a function of time. Figure (10b) shows the wave front at the top of the trapezoidal obstacle at $t=1.12$ s. At time $t=2.2$ s, the wave front is

located downstream of the obstacle (Figure (10c)). At $t=2.5$ s, the wave front arrives downstream of the channel (Figure (10d)).

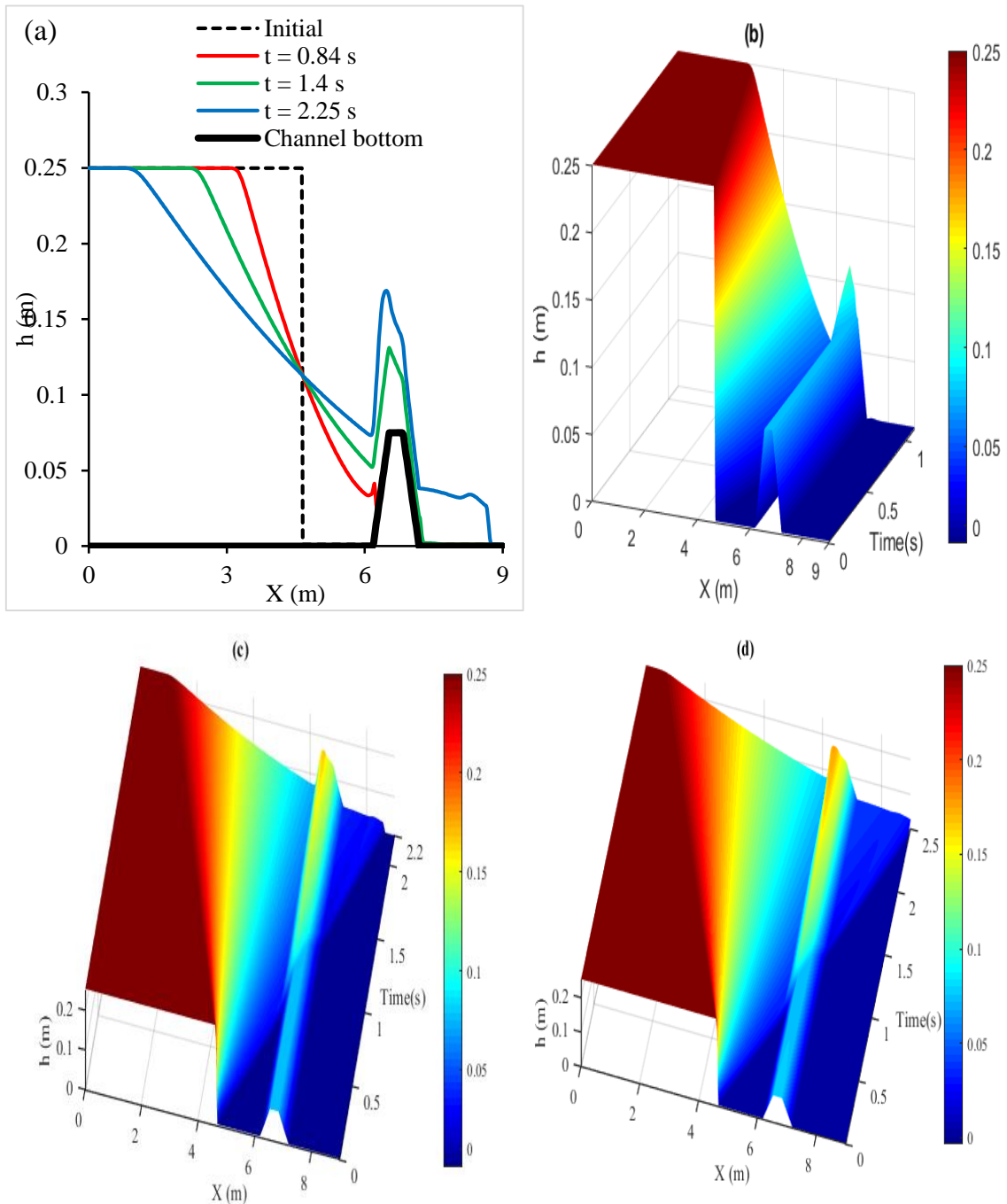


Figure (10): Displacement of the dam break wave as a function of time

Unsteady Flow in Venturi Channel

In order to study the flows due to dam failure in a contraction and expanding channel on a dry and rough bottom (with friction), a physical model was established at the LNEC (Laboratório Nacional de Engenharia Civil, Lisbon, Portugal) in collaboration with IST (Instituto

Superior Técnico) by Bento Franco et al. (1997). The initial water height is 0.3 m in the reservoir and 0.003 m downstream of the dam (Shi, 2006). The water is initially at rest, so the velocity is set to zero throughout the channel (Figure (11)).

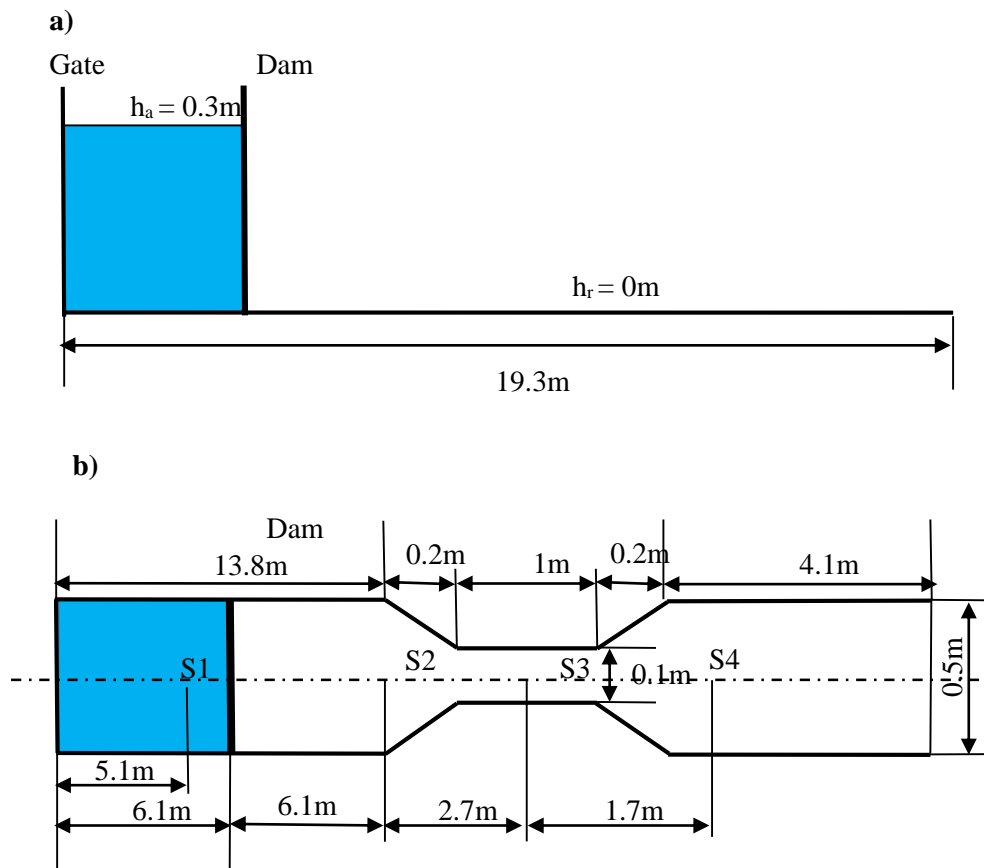


Figure (11): Channel configuration: a) Initial conditions; b) Channel geometry and measurement station positions

The four probes represent the measurement stations for the experimental and numerical data (Figure (12)). Probe S1 is located inside the reservoir 1.0m upstream of the dam. The second probe, S2, is located 6.10m downstream of the dam (just before the contraction). The third probe, S3, is located 8.8m downstream of the dam (inside the contracted section). Finally, the last probe, S4, is located in the widening section 10.50m

downstream of the dam.

Figures (12a), (12b), (12c) and (12d) show the comparison of numerical and experimental water level values for 10s at probes S1 to S4, the positions of which are given in Figure (11) and the variation of water height with varying channel width as a function of time (Figure (12e) and Figure (12f)).

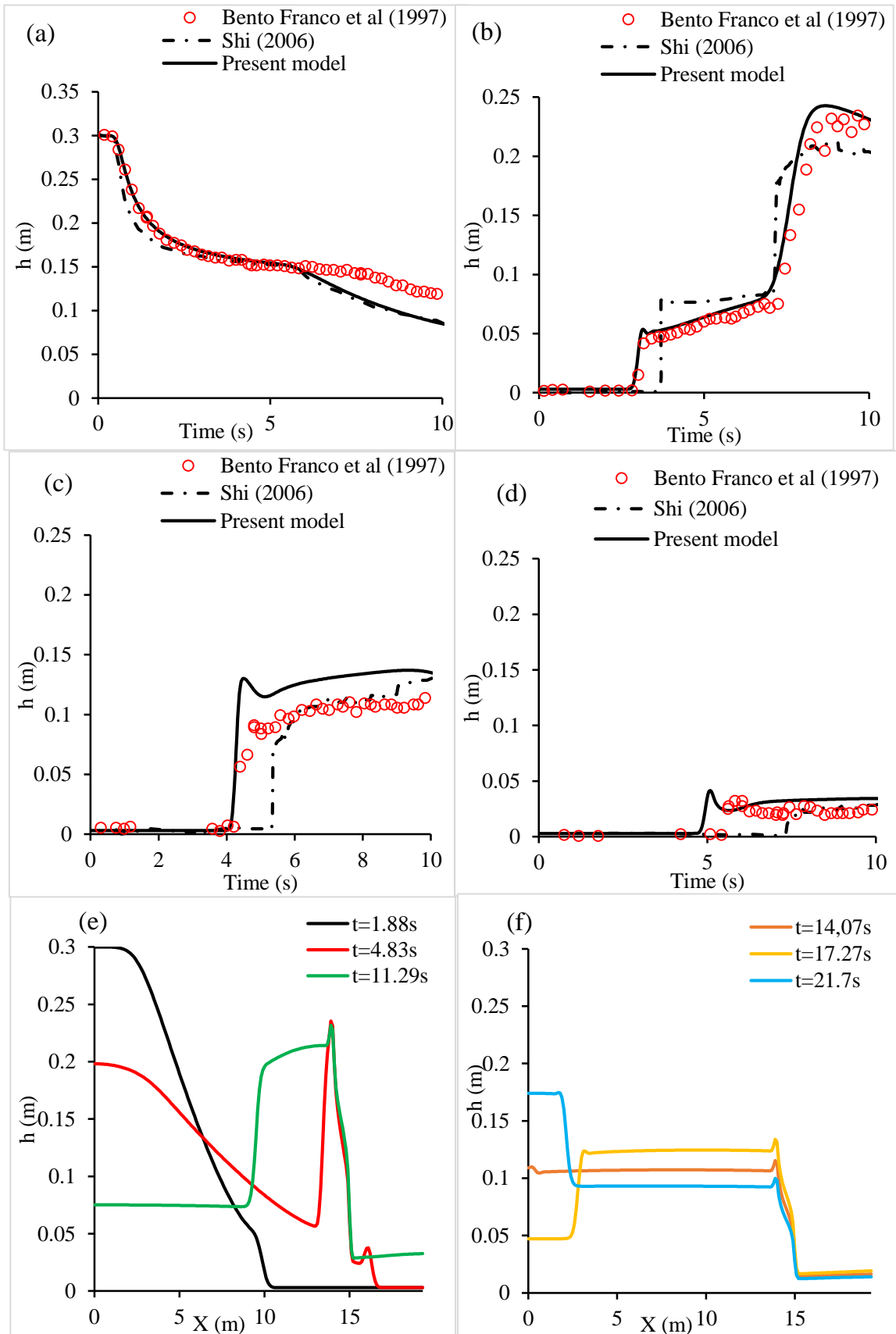


Figure (12): Variation in water depth at: a) Station S1; b) Station S2; c) Station S3; d) Station S4, and for different times

Figure (12a) shows the water height evolution in the tank at probe S1. Up to the fourth second, the numerical and experimental values are very close to each other. With the present model, the obtained results are closer to each other. The Shi numerical values (Shi, 2006), who employed the finite volume method (FVM) to solve the 2D Saint Venant equations and the present model values (computed values) then diverge, with a clear drop in the calculated free surface compared with the measured free surface.

Figure (12b) clearly shows the arrival at S2 of the shock wave due to the dam failure, which creates a reflection wave 6 s later, marked by a rise in water level. It can be seen that the arrival time of the shock wave measured and simulated with the present model is practically the same at S2. A good calibration is obtained. We note that the arrival of the shock wave at S2 calculated by Shi (2006) is one second later than the measurements. A slight offset exists between the two profiles calculated and measured at this position.

Figures (12c) and (12d) show the arrival of the shock front at probes S3 and S4. The water height value is better estimated with the present model. The arrival time of the shock wave simulated with the present model is slightly earlier than that measured (Figure (12d)). However, a delay in the arrival time of the shock wave calculated by Shi (2006) of one and two seconds, respectively, at probes S3 and S4 is observed, compared with the measurements.

Figures (12e) and (12f) show the temporal evolution of the water surface profile $h(x,t)$ within a Venturi channel at different time steps, allowing a detailed analysis of the flow behaviour in a non-prismatic geometry.

In Figure (12e), the water surface profiles are shown at $t=1.88$ s, $t=4.83$ s and $t=11.29$ s. Shortly after the start of the dam failure event, the flood wave propagates rapidly downstream, accompanied by a noticeable decrease in upstream water depth. This is a typical response in free surface flows following sudden releases, where the initial potential energy is converted into kinetic energy. At $t=4.83$ s, the flow undergoes a marked transition near the throat of the Venturi, with a noticeable drop in water level followed by a pronounced rise, due to the pressure build-up caused by the contraction. At $t=11.29$ s, the flow exhibits a quasi-steady behaviour downstream, with a residual shock

wave still visible near the outlet.

Figure (12f), show the water depth distribution at later times: $t=14.07$ s, $t=17.27$ s, and $t=21.7$ s. The water surface profile becomes increasingly structured, indicating the establishment of a steady-state flow regime in the contraction zone - characteristic of Venturi channel hydraulics. A peak in water depth is observed at the entrance to the throat, confirming the presence of a stationary wave due to the Venturi effect. This is followed by a sharp drop in depth downstream, indicating supercritical flow conditions. The observed discontinuity corresponds to a localized hydraulic jump that occurs at the transition between the contracted and the expanded sections.

Although this test case is complex and difficult to carry out, an overall agreement between the numerical computed results with the present model and the experimental values was obtained. The physical phenomenon was well reproduced by the model: the creation and propagation of a shock wave due to the rupture of the structure and then of a reflection wave due to the contraction.

CONCLUSIONS

The floods caused by dam breaks, flood events, and tsunamis are increasingly violent, and it is essential to consider with more attention the studies related to protection against this problem. Preventive measures against flooding generally consist of actions on watercourses through channel flows and infrastructure, such as protective dikes, flood control dams, or drainage systems. Implementing such protective measures requires the intervention of the hydraulic engineer in modeling and predicting the flow dynamics characterizing floods.

In this study, a numerical model based on a modified Lax-Friedrichs scheme was developed to simulate dam failure induced free surface profiles using the one-dimensional Saint Venant equations. The model effectively captured the characteristics of dam break waves in a horizontal rectangular channel with trapezoidal obstacles, achieving a relative error in water surface elevation of about 1% for ideal cases. In more complex configurations, such as Venturi-like channels, the model demonstrated high accuracy in predicting water depths and flow patterns. These results highlight

the robustness of the model in different geometric settings. Furthermore, the model offers a practical tool for preliminary flood risk assessment in dam-break scenarios. Its efficiency and simplicity make it well-suited for early decision-making, such as identifying

vulnerable areas and guiding protective design. Extending the model to 2D would enhance its ability to capture complex flows and improve its applicability to real-world flood management.

REFERENCES

- Al-Ansari, N., Adamo, N., Issa, E.I., Sissakian, V.K., and Knutsson, S. (2015). "Mystery of Mosul dam the most dangerous dam in the world: dam failure and its consequences". *Journal of Earth Sciences and Geotechnical Engineering*, 5 (3), 95-111.
- Albu, L.M., Enea, A., Iosub, M., and Breaban, I.G. (2020). "Dam breach size comparison for flood simulations. A HEC-RAS-based, GIS approach for Dracsani Lake, Sitna River, Romania." *Water*, 12 (4), 1090. <https://doi.org/10.3390/w12041090>
- Altunbilek, D. (2002). "The role of dams in development". *Water Resources Development*, 18 (1), 9-24.
- Annunziato, A., Santini, M., Proietti, C., de Girolamo, L., Lorini, V., Gerhardinger, A., and Tucci, M. (2024). "Modeling and validation of the Derna dam break event". *GeoHazards*, 5 (2), 504-529. <https://doi.org/10.3390/geohazards5020026>
- Baghlani, A. (2011). "Simulation of dam-break problem by a robust flux-vector splitting approach in Cartesian grid." *Scientia Iranica A*, 18 (5), 1061-1068. <https://doi.org/10.1016/j.scient.2011.09.004>
- Bento Franco, A., Betâmio de Almeida, A., and Viseu, T. (1997). "Dam break in a channel with a local constriction." *WGDM Belgium Meeting*.
- Chaudhry, M.H. (2008). "Open-channel flow".
- Das, R., and Bagheri, S. (2015). "A robust numerical scheme for simulating unsteady open channel flows." *J. Hydraul. Res.*, 53(6), 739-751.
- Delloum, W., Bouderah, B., and Bounab, N. (2024). "Approximate analytic solution of a potential flow around an obstacle". *Math. Model. Eng. Probl.*, 11 (8). <https://doi.org/10.18280/mmep.110827>
- Elhakeem, M. (2017). "Explicit solution for flow depth in open channels of trapezoidal cross-sectional area: Classic problem of interest". *J. Irrig. Drain. Eng.*, 143, 04017011. [https://doi.org/10.1061/\(ASCE\)IR.1943-4774.000117](https://doi.org/10.1061/(ASCE)IR.1943-4774.000117)
- Garcia-Navarro, P., Frás, A., and Villanueva, I. (1999). "Dam-break flow simulation: Some results for one-dimensional models of real cases." *Journal of Hydrology*, 216, 227-247. [https://doi.org/10.1016/S0045-7930\(99\)00038-9](https://doi.org/10.1016/S0045-7930(99)00038-9)
- Garcia-Navarro, P., and Vazquez-Cendon, M.E. (2000). "On numerical treatment of the source terms in the shallow-water equations." *Computers & Fluids*, 29, 951-979.
- Helfrich, K.R., Allen, C.K., and Pratt, L.J. (1999). "Nonlinear Rossby adjustment in a channel." *Journal of Fluid Mechanics*, 390, 187-222. <https://doi.org/10.1017/S0022112099005042>
- Huang, J., and Song, C.C. (1985). "Stability of dynamic flood routing schemes". *Journal of Hydraulic Engineering*, 111 (12), 1497-1505.
- Ikni, T., Berreksi, A., and Belhocine, M. (2021). "Numerical study of shallow-water equations using three explicit schemes: Application to dam-break flood wave." *International Journal of Hydrology Science and Technology*, 12 (2), 101-115. <https://doi.org/10.1504/IJHST.2021.116662>
- Ikni, T., Berreksi, A., Hamidou, M., Belhocine, M., Nebbar, M.L., and Benkadja, R. (2018). "Contribution to the study of the dam-break wave propagation via finite differences formulations." *Larhyss Journal*, 33, 169-188.
- Lacasta, A., Morales-Hernández, M., Brufau, P., and Garcia-Navarro, P. (2017). "Application of an adjoint-based optimization procedure for the optimal control of internal boundary conditions in the shallow-water equations". *Journal of Hydraulic Research*, 56, 1-13. <https://doi.org/10.1080/00221686.2017.1300196>
- Leveque, R.J. (1992) "Numerical methods for conservation law". Birkhauser Verlag, Germany. <https://doi.org/10.1007/978-3-0348-8629-1>
- Magdalena, I., and Pebriansyah, M.F.E. (2022). "Numerical treatment of finite difference method for solving dam-break model on a wet-dry bed with an obstacle." *Results in Engineering*, 14, 100-382. <https://doi.org/10.1016/j.rineng.2022.100382>

- Mohapatra, P.K., and Murty Bhallamudi, S. (1996). "Computation of a dam-break flood wave in channel transitions." *Adv. Water Resour.*, 19 (3), 181-187. [https://doi.org/10.1016/0309-1708\(95\)00036-4](https://doi.org/10.1016/0309-1708(95)00036-4)
- Nema, M., and Desmukh, T.S. (2016). "Dam break: A review." *International Journal of Advanced Engineering Research and Science*, 3 (6).
- Oguzhan, S., and Aksoy, A.O. (2020). "Experimental investigation of the effect of vegetation on dam-break flood waves." *Journal of Hydrology and Hydromechanics*, 68 (3), 231-241. <https://doi.org/10.2478/johh-2020-0026>
- Ozmen-Cagatay, H., and Kocaman, S. (2011). "Dam-break flow in the presence of obstacle: Experiment and CFD simulation." *Engineering Applications of Computational Fluid Mechanics*, 5 (4), 541-552. <https://doi.org/10.1080/19942060.2011.11015393>
- Paşa, Y., Peker, I.B., Haci, A., and Gülbaz, S. (2023). "Dam-failure analysis and flood-disaster simulation under various scenarios." *Water Science & Technology*, 00 (0), 1. <https://doi.org/10.2166/wst.2023.052>
- Saikia, M.D., and Sarma, A.K. (2006). "Analysis for adopting logical channel section for 1D dam-break analysis in natural channels." *ARPJ Journal of Engineering and Applied Sciences*, 1 (2), 46-54.
- Sanjoyo, B., Hariadi, M., and Purnomo, M.H. (2020). "Stable algorithm Based on Lax-Friedrichs scheme for visual simulation of shallow water". *EMITTER International Journal of Engineering Technology*, 8 (1), 19-34. <https://doi.org/10.24003/emitter.v8i1.479>
- Sawai, A., Shyamal, D.S., and Kumar, L. (2019). "Dam-break analysis: A review of literature." *International Journal of Research in Engineering Application and Management*, 4 (12), 538-542. <https://doi.org/10.18231/2454-9150.2019.0183>
- Shatnawi, N. (2024). "Mapping floods during cloudy weather using radar satellite images." *Jordan J. Civ. Eng.*, 18. <https://doi.org/10.14525/JJCE.v18i1.03>
- Shi, Yu-E. (2006). "Résolution numérique des équations de Saint-Venant par la technique de projection en utilisant une méthode des volumes finis dans un maillage non structuré." *Sciences de la Terre, Université de Caen*. <https://tel.archives-ouvertes.fr/tel-00130539v2>
- Stoker, J.J. (1957). "Water waves." *Interscience Publishers, Inc., Wiley and Sons, New York, U.S.A.*
- Townson, J.M., and Al-Salihi, A.H. (1989). "Models of dam-break flow in R-T space." *J. Hydraul. Eng., ASCE*, 115 (5), 561-575.
- Welahettige, P., Lie, B., and Vaagsaether, K. (2017). "Computational fluid dynamics study of flow depth in an open Venturi channel for Newtonian fluid." *Proc. 58th Conf. on Simulation and Modling (SIMS 58)*, Sept. 25-27. 29-34. *Linköping University Electronic Press, Sweden, Reykjavik, Iceland*. <https://doi.org/10.3384/ecp1713829>